J|A|C|S
ARTICLES
Published on Web 09/02/2004

Theoretical Study on the Photochromic Cycloreversion Reactions of Dithienylethenes; on the Role of the Conical Intersections

Yukako Asano,[†] Akinori Murakami,[‡] Takao Kobayashi,[‡] Alexander Goldberg,[‡] Dominique Guillaumont,[‡] Satoshi Yabushita,*[,†] Masahiro Irie,[§] and Shinichiro Nakamura*[,‡]

Contribution from the Department of Chemistry, Faculty of Science and Technology, Keio University, 3-14-1 Hiyoshi, Kohoku-ku, Yokohama 223-8522, Japan, Mitsubishi Chemical Corporation, MCC-Group Science and Technology Research Center Inc., 1000 Kamoshida-cho, Aoba-ku, Yokohama 227-8502, Japan, and Department of Chemistry and Biochemistry, Graduate School of Engineering, Kyushu University, Hakozaki 6-10-1, Higashi-ku, Fukuoka 812-8581, Japan

Received March 6, 2003; E-mail: shin@rc.m-kagaku.co.jp

Abstract: The mechanism of the photochromic cycloreversion reactions is theoretically examined in a model system of dithienylethenes by means of the CASSCF and CASPT2 methods. The structures of its conical intersections (CIs), which are the branching points of the internal conversions, were obtained. The analyses of the minimum energy paths from the Franck−Condon states and the CI points suggest that the cycloreversion reaction occurs during the intramolecular vibrational energy redistribution (IVR) toward the quasi-equilibrium on the 2A state. The current study of the model system will provide a basic insight for the photochromic molecular design.

1. Introduction

Photochromism is defined as a reversible transformation between two isomers by photoirradiation.[1,2] Dithienylethenes with heterocyclic aryl groups show photochromism and have recently attracted much attention because of their potential application to optoelectronic devices, such as optical memories and optical switches.[3−5] For such applications, both cyclization and cycloreversion reactions should have large quantum yields (QYs) as well as large absorption maxima to be able to control their properties.

Many groups have experimentally investigated the dynamics for the cyclization[6−9] and cycloreversion[11−13] reactions of various dithienylethene derivatives. For example, Miyasaka et al.[6] observed that the efficiency of the cycloreversion reaction in bis (2-methyl-5-phenylthiophen-3-yl) perfluorocyclopentene is dramatically enhanced by irradiation with a picosecond laser. They concluded that the stepwise multiphoton process results in an efficient production of the open-ring isomer. Reported time constants of the cycloreversion reactions depend on the compounds and vary from 2.1 ps[11] and <10 ps[12] to 325 ps,[13] while those for the cyclization reactions are independent of the compounds. Also, there are no slow radiation processes such as fluorescence in most cycloreversion reactions. These experimental facts suggest the existence of very fast internal conversion (IC) processes, that is, conical intersections (CIs).

Reaction mechanisms via CIs have recently been studied extensively in various kinds of photochemical reactions. In the early 1990s, Robb et al.[14] theoretically studied the photochemical transformation mechanism of butadiene and replaced the Oosterhoff model[15] with their reaction mechanism based on the CIs. They showed the two reasons for the very existence of the CIs: the efficient radiationless transition from the excited ($2\ ^1A_g$) to ground ($1\ ^1A_g$) state and the presence of different photoproducts from the same precursor.

[†] Keio University.
[‡] Mitsubishi Chemical Corp.
[§] Kyushu University.

(1) Bouas-Laurent, H. In *PHOTOCHROMISM Molecules and Systems*; Dürr, H., Ed.; Elsevier: Amsterdam, 1990.
(2) Crano, J. C., Gugielmetti, R. J., Eds.; *Organic Photochromic and Thermochromic Compounds*; Plenum: New York, 1999; see also Chapter 5 for Molecular Modeling Calculations.
(3) Irie, M. *Chem. Rev.* **2000**, *100*, 1685.
(4) Tamai, N.; Miyasaka, H. *Chem. Rev.* **2000**, *100*, 1875.
(5) Gilat, S. L.; Kawai, S. H.; Lehn, J.-M. *Chem.-Eur. J.* **1995**, *1*, 275.
(6) Kaieda, T.; Kobatake, S.; Miyasaka, H.; Murakami, M.; Iwai, N.; Nagata, Y.; Itaya, A.; Irie, M. *J. Am. Chem. Soc.* **2002**, *124*, 2015.
(7) Miyasaka, H.; Nobuto, T.; Itaya, A.; Tamai, N.; Irie, M. *Chem. Phys. Lett.* **1997**, *269*, 281.
(8) Owrutsky, J. C.; Nelson, H. H.; Baronavski, A. P.; Kim, O.-K.; Tsivgoulis, G. M.; Gilat, S. L.; Lehn J.-M. *Chem. Phys. Lett.* **1998**, *293*, 555.
(9) Hania, P. R.; Lucas, L. N.; Pugzlys, A.; van Esch, J.; Feringa, B. L.; Snijders, J. G.; Duppen, K. *J. Phys. Chem. A* **2002**, *106*, 8498.
(10) Miyasaka, H.; Murakami, M.; Itaya, A.; Guillaumont, D.; Nakamura, S.; Irie, M. *J. Am. Chem. Soc.* **2001**, *123*, 753.
(11) Ern, J.; Bens, A. T.; Bock, A.; Martin, H.-D.; Kryschi, C. *J. Lumin.* **1998**, *76*/*77*, 90.
(12) Miyasaka, H.; Araki, S.; Tabata, A.; Nobuto, T.; Mataga, N.; Irie, M. *Chem. Phys. Lett.* **1994**, *230*, 249.
(13) Ern, J.; Bens, A. T.; Martin, H.-D.; Mukamel, S.; Schmid, D.; Tretiak, S.; Tsiper, E.; Kryschi, C. *Chem. Phys.* **1999**, *246*, 115.
(14) (a) Olivucci, M.; Ragazos, I. N.; Bernardi, F.; Robb, M. A. *J. Am. Chem. Soc.* **1993**, *115*, 3710. (b) Boggio-Pasqua, M.; Ravaglia, M.; Bearpark, M. J.; Garavelli, M.; Robb, M. A. *J. Phys. Chem. A* **2003**, *107*, 11139. This paper appeared as the first ab initio report of the CIs for dithienylethene derivatives, while we were preparing the revised version.
(15) van der Lugt, W. T. A. M.; Oosterhoff, L. J. *J. Am. Chem. Soc.* **1969**, *91*, 6042.

10.1021/ja035035o CCC: $27.50 **© 2004 American Chemical Society**

Scheme 1

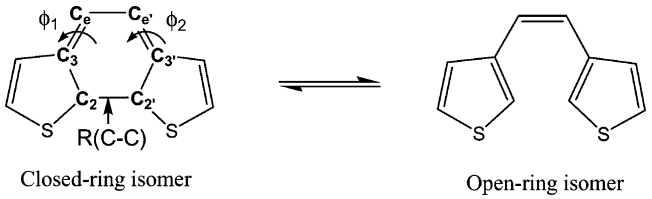

They[16−18] have also theoretically studied the CIs in several isomerization reactions of relatively large compounds. In particular, they[16,17] reported a very interesting study on the CI structures between the S_0 ($1A_1$) and S_1 ($2A_1$) states of cyclohexa-1,3-diene, which is the central framework of the current dithienylethenes. Kryschi et al.[13,19,20] examined the dynamics for the cyclization and cycloreversion reactions of some dithienylethene derivatives using the INDO/S semiempirical Hamiltonian. They suggested the existence of a CI as a branching point to the closed- or open-ring isomers and discussed that the radiationless deactivation and branching processes take place competitively from the precursor of the reaction. However, because of the heavy computations, the CI structures of dithienylethenes have been scarcely[14b] obtained with ab initio methods, even though they are indispensable for analyzing the reaction mechanisms.

We have been investigating photochromic molecules,[2] in an attempt to provide the principles for molecular design with various functional properties for many applications;[2,3] in particular, the QY was theoretically studied on a model system of dithienylethenes[21] shown in Scheme 1. This was an extension of a previous study on thermal stability[22a] which is an important property implying the system can be operative only by photons, as is understood by the Woodward−Hoffmann rules. The photochromic cycloreversion reaction occurs via the HOMO−LUMO ($\pi \rightarrow \pi^*$) single-excitation state corresponding to the excitation from the 1A to 1B state at the closed-ring isomer under the C_2 symmetry (see Figure 1).[21,22] After the excitation, the open-ring isomer is produced via some IC processes. For an understanding of experimental QYs in line with the Woodward−Hoffmann rules, an investigation of the detailed mechanism was in order. In a previous paper,[21] we have theoretically shown that the energy difference between the closed- ($2A_C$) and open-ring ($2A_O$) isomers on the 2A state (the subscripts C and O represent the closed- and open-ring isomers, respectively) is correlated with the experimental QYs of the cycloreversion reaction. It is very useful to observe such a good correlation for a practical guide; however, for further advances, the theoretical rationalization is necessary by explicitly taking IC processes into account.

This paper presents an ab initio MO study to explore the cycloreversion reaction mechanism in a model system of dithienylethenes focusing on the CIs. We have calculated the potential energy surfaces (PESs), important CI structures and their characters, and the minimum energy paths (MEPs), using the CASSCF and CASPT2 method. The purpose of this paper is to provide the basic framework of the mechanism in photochromic cycloreversion reactions, toward the insight for the QY design in real dithienylethene molecules.

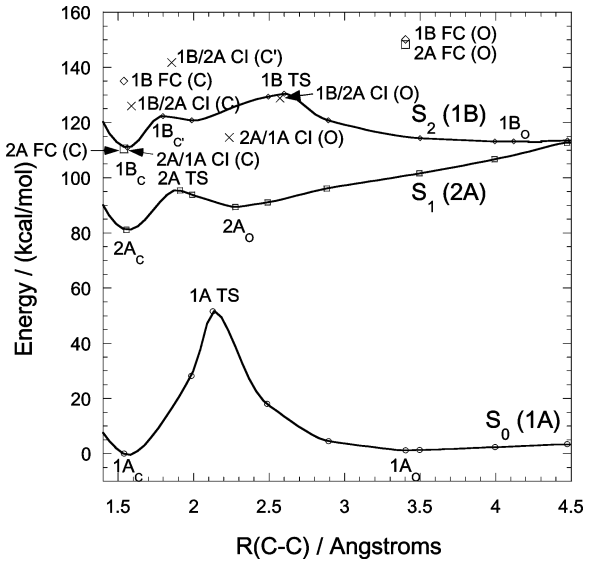

Figure 1. Potential energy surfaces of the ground (1A) and two lower excited (2A and 1B) states as a function of the distance between the two reactive carbon atoms, R(C−C). The symbol i/j represents the conical intersection (CI) point between the states i and j in the C_2 symmetry notation, and the letters in parentheses, C and O, represent the closed- and open-ring structures, respectively.

2. Computational Methods

We used the 6-31G basis sets and the complete active space self-consistent-field (CASSCF) method as before[21] for the most part. The active space of CASSCF (10,10) was employed, where the numbers of electrons and orbitals are respectively represented in parentheses, 10 electrons in the 10π orbitals for the open-ring isomers. For the closed-ring isomers, the 10 orbitals correspond to the 2σ and 8π orbitals. To check the dynamical correlation effect and the basis set dependency, the additional single-point calculations of CASSCF (14,14) with the active space including four more σ electrons and σ orbitals of the C−S bonds, as well as CASSCF (10,10) with the 6-31G* basis sets and CASPT2 (10,10), were also carried out.

For the ground (1A) and two lower excited (2A and 1B) states, we calculated the PESs as a function of R(C−C) and the minimum structures under the C_2 symmetry. The R(C−C) is defined by the distance between the two reactive carbon atoms (see Scheme 1). The optimized C_2 structures were verified to be local minima by the frequency analysis.

Without the symmetry restriction, we determined some important CI structures located between the 1A and 2A states, and between the 2A and 1B states. The MEPs from the Franck−Condon (FC) states (i.e., vertically excited states) and from the CI points to the stable structures were calculated to examine the geometry changes during the cycloreversion reaction. They

(16) (a) Celani, P.; Ottani, S.; Olivucci, M.; Bernardi, F.; Robb, M. A. *J. Am. Chem. Soc.* **1994**, *116*, 10141. (b) Celani, P.; Bernardi, F.; Robb, M. A.; Olivucci, M. *J. Phys. Chem.* **1996**, *100*, 19364.
(17) Garavelli, M.; Page, C. S.; Celani, P.; Olivucci, M.; Schmid, W. F.; Trushin, S. A.; Fuss, W. *J. Phys. Chem. A* **2001**, *105*, 4458.
(18) Boggio-Pasqua, M.; Bearpeak, M. J.; Hunt, P. A.; Robb, M. A. *J. Am. Chem. Soc.* **2002**, *124*, 1456.
(19) Ern, J.; Bens, A. T.; Martin, H.-D.; Mukamel, S.; Schmid, D.; Tretiak, S.; Tsiper, E.; Kryschi, C. *J. Lumin.* **2000**, *87*, 742.
(20) Ern, J.; Bens, A. T.; Martin, H.-D.; Kuldova, K.; Trommsdorff, H. P.; Kryschi, C. *J. Phys. Chem. A* **2002**, *106*, 1654.
(21) Guillaumont, D.; Kobayashi, T.; Kanda, K.; Miyasaka, H.; Uchida, K.; Kobatake, S.; Shibata, K.; Nakamura, S.; Irie, M. *J. Phys. Chem. A* **2002**, *106*, 7222.
(22) (a) Nakamura, S.; Irie, M. *J. Org. Chem.* **1988**, *53*, 6136. (b) Uchida, K.; Guillaumont, D.; Tsuchida, E.; Mochizuki, G.; Irie, M.; Murakami, A.; Nakamura, S. *J. Mol. Struct. (THEOCHEM)* **2002**, *579*, 115.

are not the usual intrinsic reaction coordinates (IRCs), because the gradients are not zero at the starting points. We, therefore, performed the quasi-IRC calculations by tracing the steepest descent paths from these points in the mass-weighted Cartesian coordinate system. We used the GAMESS,[23] MOLCAS,[24] and MOLPRO[25] program packages.

3. Results and Discussion

3.1. Adiabatic Potential Energy Profiles. Figure 1 shows the adiabatic PESs with CASSCF (10,10) for the ground (1A) and two lower excited (2A and 1B) states as a function of R(C−C) under the C_2 symmetry (Table 1). The minimum and transition state structures were reported in a previous paper.[21]

For examining the geometry changes during the cycloreversion reaction, we show in Figure 2 the MEPs from a transition state on the 1A PES (1A TS), and from the 2A and 1B FC states at the $1A_C$ and $1A_O$ structures. Figure 2a and b shows the MEPs projected on R(C−C) and the torsion angles about the cyclohexane ring ϕ, respectively. The torsion angles ϕ_1 and ϕ_2 are defined by the dihedral angles ∠2−3−e−e′ and ∠2′−3′−e′−e, respectively (see Scheme 1), and ϕ is equal to ϕ_1 and ϕ_2 under the C_2 symmetry.

As shown in Figure 2a, R(C−C) is not always a good reaction coordinate, in particular, for the MEPs from the FC states at the $1A_C$ and $1A_O$ structures, while it is a good reaction coordinate for the MEPs from 1A TS. On the other hand, ϕ can be a good reaction coordinate for all of the MEPs as shown in Figure 2b.[26] We will express all of the geometries by R(C−C), ϕ_1, and ϕ_2, hereafter. Figure 3 summarizes the geometrical parameters R(C−C) and ϕ for all of the important structures.

3.2. Conical Intersections. We describe here the characteristics of CIs prior to the discussion on the mechanism of the cycloreversion reaction. The noncrossing rule[27] has been established in diatomic molecules. On the other hand, in a polyatomic system such as dithienylethenes, it has been theoretically revealed[28] that the noncrossing rule does not hold, and two electronic states even with the same spatial and spin symmetries can cross. A CI point corresponds to the energy minimum along the crossing seam, where the transition from the upper to lower state can occur most efficiently, as shown in Scheme 2. The reaction path just after the transition lies in the branching plane defined by the two vectors: the gradient difference vector $\boldsymbol{x}_1$ and the derivative coupling vector $\boldsymbol{x}_2$.

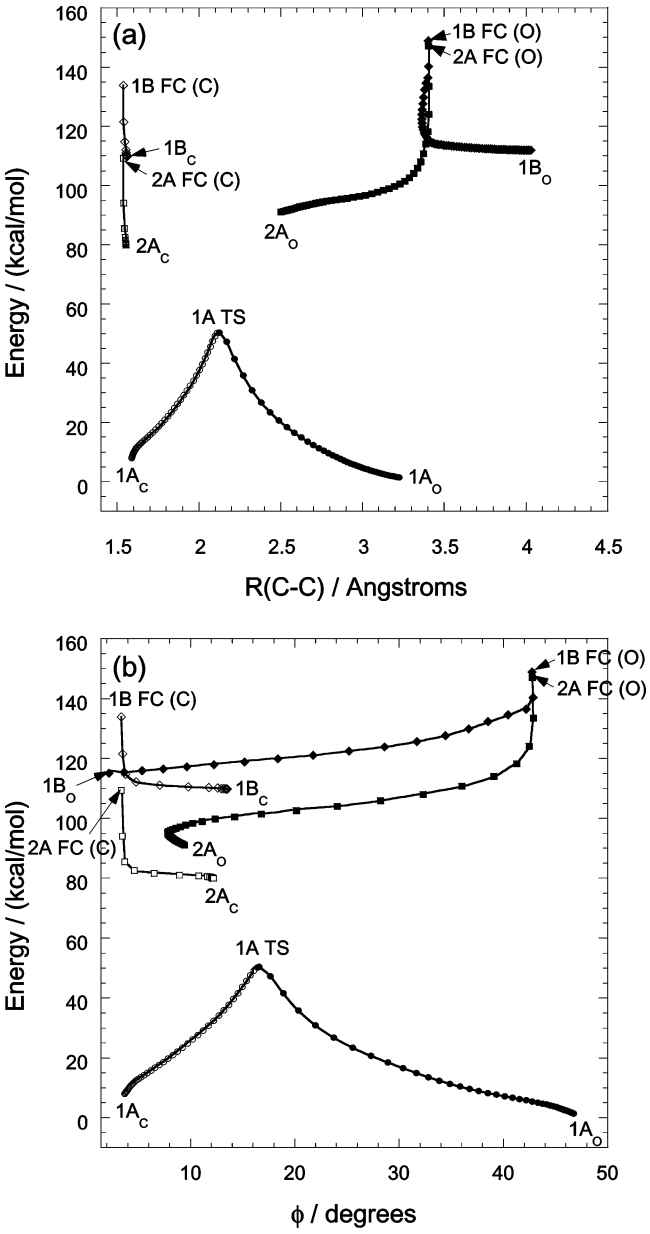

Figure 2. (a) The minimum energy paths (MEPs) projected on the distance between the two reactive carbon atoms, R(C−C), from the geometry for the transition state of the 1A state (1A TS), and the 2A and 1B Franck−Condon (FC) states at the closed- ($1A_C$) and open-ring structures ($1A_O$) of the 1A state, 2A FC (C), 2A FC (O), 1B FC (C), and 1B FC (O). (◇): The path from 1B FC (C) to $1B_C$. (□): The path from 2A FC (C) to $2A_C$. (◆): The path from 1B FC (O) to $1B_O$. (■): The path from 2A FC (O) to $2A_O$. (○): The path from 1A TS to $1A_C$. (●): The path from 1A TS to $1A_O$. (b) The minimum energy paths (MEPs) projected on the torsion angle about the cyclohexane ring ϕ. The two torsion angles ϕ_1 and ϕ_2 are equal to ϕ because of the C_2 symmetry. The same symbols as in Figure 2a are used.

Therefore, a CI has an infinite number of reaction path directions in this branching plane;[28] by contrast, a transition state for the thermal reaction gives only one direction for the MEP. These different reaction paths may result in different final products, and thus a CI acts as a branching point.[14,16−18,28−30]

The structures of the optimized CIs are shown in Figure 4a, together with $\boldsymbol{x}_1$ and $\boldsymbol{x}_2$ vectors in Figure 4b (Table 2). The

(23) Schmidt, M. W.; Baldridge, K. K.; Boatz, J. A.; Elbert, S. T.; Gordon, M. S.; Jensen, J. H.; Koseki, S.; Matsunaga, N.; Nguyen, K. A.; Su, S. J.; Windus, T. L.; Dupuis, M.; Montgomery, J. A. *J. Comput. Chem.* **1993**, *14*, 1347.
(24) Andersson, K.; Barysz, M.; Bernhardsson, A.; Blomberg, M. R. A.; Carissan, Y.; Cooper, D. L.; Cossi, M.; Fleig, T.; Fülscher, M. P.; Gagliardi, L.; de Graaf, C.; Hess, B. A.; Karlström, G.; Lindh, R.; Malmqvist, P.-Å.; Neogrády, P.; Olsen, J.; Roos, B. O.; Schimmelpfennig, B.; Schütz, M.; Seijo, L.; Serrano-Andrés, L.; Siegbahn, P. E. M.; Stålring, J.; Thorsteinsson, T.; Veryazov, V.; Wierzbowska, M.; Widmark, P.-O. *MOLCAS 5.1*; Lund University: Sweden, 2001.
(25) Werner, H.-J.; Knowles, P. J. *MOLPRO 2000.1*; University of Birmingham.
(26) In Figure 2a and b, the minimum energy paths (MEPs) just stemming from the Franck−Condon (FC) states at the $1A_C$ and $1A_O$ structures show only small geometry changes for both R(C−C) and ϕ; in this region, there occur bond alternations from the ground- to excited-state structures. For general instructive references, see: Olivucci, M.; Robb, M. A.; Bernardi, F. Calculations of Excited-state Conformational Properties. In *Conformational Analysis of Molecules in Excited States*; Waluk, J., Ed.; Wiley-VCH: New York, 2000; p 297.
(27) von Neumann, J.; Wigner, E. *Phys. Z.* **1929**, *30*, 467.
(28) (a) Yarkony, D. R. *J. Phys. Chem. A* **2001**, *105*, 6277. (b) Yarkony, D. R. *J. Chem. Phys.* **2001**, *114*, 2601. (c) Yarkony, D. R. *Rev. Mod. Phys.* **1996**, *68*, 985. (d) Atchity, G. J.; Xantheas, S. S.; Ruedenberg, K. *J. Chem. Phys.* **1991**, *95*, 1862.
(29) Ragazos, I. N.; Robb, M. A.; Bernardi, F.; Olivucci, M. *Chem. Phys. Lett.* **1992**, *197*, 217.
(30) Garavelli, M.; Celani, P.; Fato, M.; Bearpark, M. J.; Smith, B. R.; Olivucci, M.; Robb, M. A. *J. Chem. Phys.* **1997**, *101*, 2023.

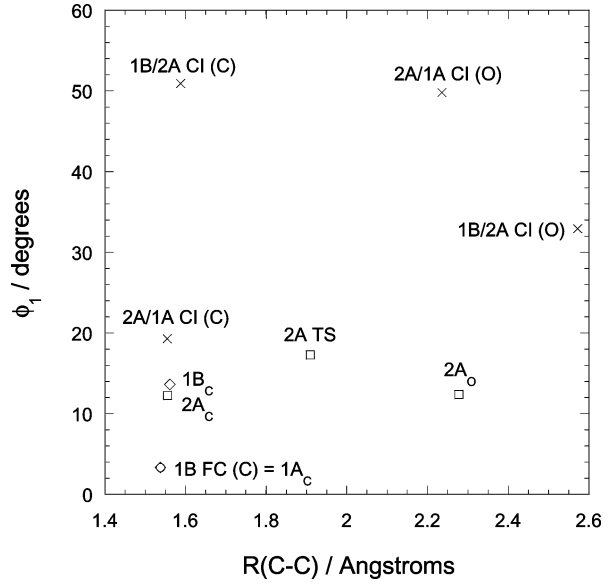

Figure 3. Summary of the geometrical parameters R(C−C) and ϕ_1 for all of the important structures to discuss the mechanism of the cycloreversion reaction. Note that the initial relaxation from the 1B FC state induces the twisting motion of the thienyl groups. Internal conversions through the conical intersections require the same molecular deformation represented by the change in the dihedral angle ϕ_1. The reaction coordinate from $2A_C$ to $2A_O$ is perpendicular to the ϕ_1 axis; therefore, the intramolecular vibrational energy redistribution (IVR) is required for the cycloreversion reaction.

Scheme 2

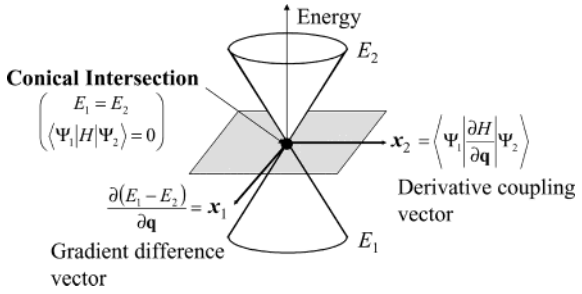

symbol *i*/*j* represents the CI point between the upper state *i* and the lower state *j* in the C_2 symmetry notation, and the letters in parentheses, C and O, represent the closed- and open-ring structures, respectively. Although ϕ_1 and ϕ_2 in the optimized CIs are different from each other and their structures are distorted from the C_2 symmetry, the states are expressed in the C_2 symmetry notation for an aid in understanding.

It is noted here that the central framework of 2A/1A CI (O) is very similar to the CI structure between the S_0 ($1A_1$) and S_1 ($2A_1$) states of cyclohexa-1,3-diene calculated by Robb et al.[16] and Garavelli et al.[17] Noted also is that neither the CASSCF (6,6) nor CASSCF (8,8) method can produce the similar CI structure. Therefore, the selection of the appropriate active space is crucial, in particular, in the determination of the correct torsion angles about the cyclohexane ring, and at least the CASSCF (10,10) method must be chosen.[21] As summarized in Figures 3 and 4a, all of the CIs except for 1B/2A CI(C′) have a common structural feature in that only one of the two thienyl groups has a fairly large dihedral angle ϕ_1.[14b]

Kryschi et al.[13] investigated the dynamics for the cycloreversion reaction of 1,2-bis (5-formyl-2-methyl-thien-3-yl) perfluorocyclopentene by using the collective electronic oscillator approach with the INDO/S semiempirical Hamiltonian. Their R(C−C) values for the S_0 closed-ring isomer (1.54 Å), the S_0 open-ring isomer (3.93 Å), a potential barrier on the S_1 surface (1.80 Å), and the S_1/S_0 CI (2.15 Å) are similar to our values for the current compound,[21] 1.537, 3.402, 1.909, and 2.235 Å, respectively (Figures 1 and 4a).

The local topography of the PESs near the CI structure in Scheme 2 is the simplest one, and the actual structure can be significantly deformed; the two PESs together form an elliptical cone with a largely tilted axis against the energy axis.[28] Table 3 shows the conical parameters defined by Yarkony,[28a,b] to represent the local topography in the vicinity of the CIs. In obtaining these parameters, the $\boldsymbol{x}_1$ and $\boldsymbol{x}_2$ vectors have been orthogonalized into $\boldsymbol{x}_{1'}$ and $\boldsymbol{x}_{2'}$ vectors by using the Yarkony procedure. A CI with the tilt parameter $|s^x| < 1$ ($|s^y| < 1$) can be classified as a peaked type along the $\boldsymbol{x}_{1'}$ ($\boldsymbol{x}_{2'}$) direction, while one with $|s^x| > 1$ ($|s^y| > 1$) can be classified as a sloped type along the $\boldsymbol{x}_{1'}$ ($\boldsymbol{x}_{2'}$) direction. 2A/1A CI(C) and 1B/2A CI(O) are characterized as intermediate types along both the $\boldsymbol{x}_{1'}$ and the $\boldsymbol{x}_{2'}$ directions, while 1B/2A CI(C′) is characterized as peaked and sloped types along the $\boldsymbol{x}_{1'}$ and $\boldsymbol{x}_{2'}$ directions, respectively. The characters of 1B/2A CI(C) and 2A/1A CI(O) are of critical importance for the photochromic reaction mechanism (Figure 1) and will be discussed later.

Figure 5a and b focuses on the potential energy in the vicinity of 1B/2A CI(C) and 2A/1A CI (O), respectively. Each of the upper parts compares the two kinds of potential energy changes along a circle with a radius of 0.01 bohr around the CI on the branching plane, one obtained from the actual pointwise CASSCF calculations and the other from the degenerate perturbation theory estimate with the conical parameters. In both CIs, the agreement between the results from the pointwise calculations and the perturbation theory estimate is fairly good. Lower parts illustrate the three-dimensional views of the S_2/S_1 (or S_1/S_0) PESs in the branching plane around the CIs, which have been obtained from the perturbation theory estimate. As shown in Figure 5a, 1B/2A CI(C) is characterized as a distinctly sloped type along the $\boldsymbol{x}_{1'}$ direction and a slightly peaked type along the $\boldsymbol{x}_{2'}$ direction, which can be also confirmed by the tilt parameters s^x and s^y shown in Table 3. The structures of both $1B_C$ and $2A_C$ are located in the negative side of the $\boldsymbol{x}_2$ coordinate, with the smaller dihedral angles ϕ_1 (Figure 3); thus a very efficient IC from the 1B to 2A state is expected to occur at 1B/2A CI(C). As we will describe later, all of the MEPs from this CI point led to $2A_C$ without branching. In Figure 5b, it is shown that the PES topography of 2A/1A CI (O) is a peaked type along the $\boldsymbol{x}_{1'}$ direction, while it is an intermediate type along the $\boldsymbol{x}_{2'}$ direction, which has been also verified by the tilt parameters (s^x and s^y). This topography suggests the 2A/1A CI(O) point would play a role of a branching point leading to different stable products.

Figure 6 represents the results of the MEPs from the CI points. We showed only one MEP from each of the 1B/2A CI (C), 1B/2A CI (C′), 1B/2A CI (O), and 2A/1A CI (C) points. Such MEPs belong to the lower branch of PES near the CI points. We have also traced the MEPs starting from several structures that were slightly apart from these CI points on the branching planes. As far as we examined, all of the MEPs from each of the CI points arrived at the same final product with similar MEPs, except from the 2A/1A CI (O) point. This 2A/1A CI

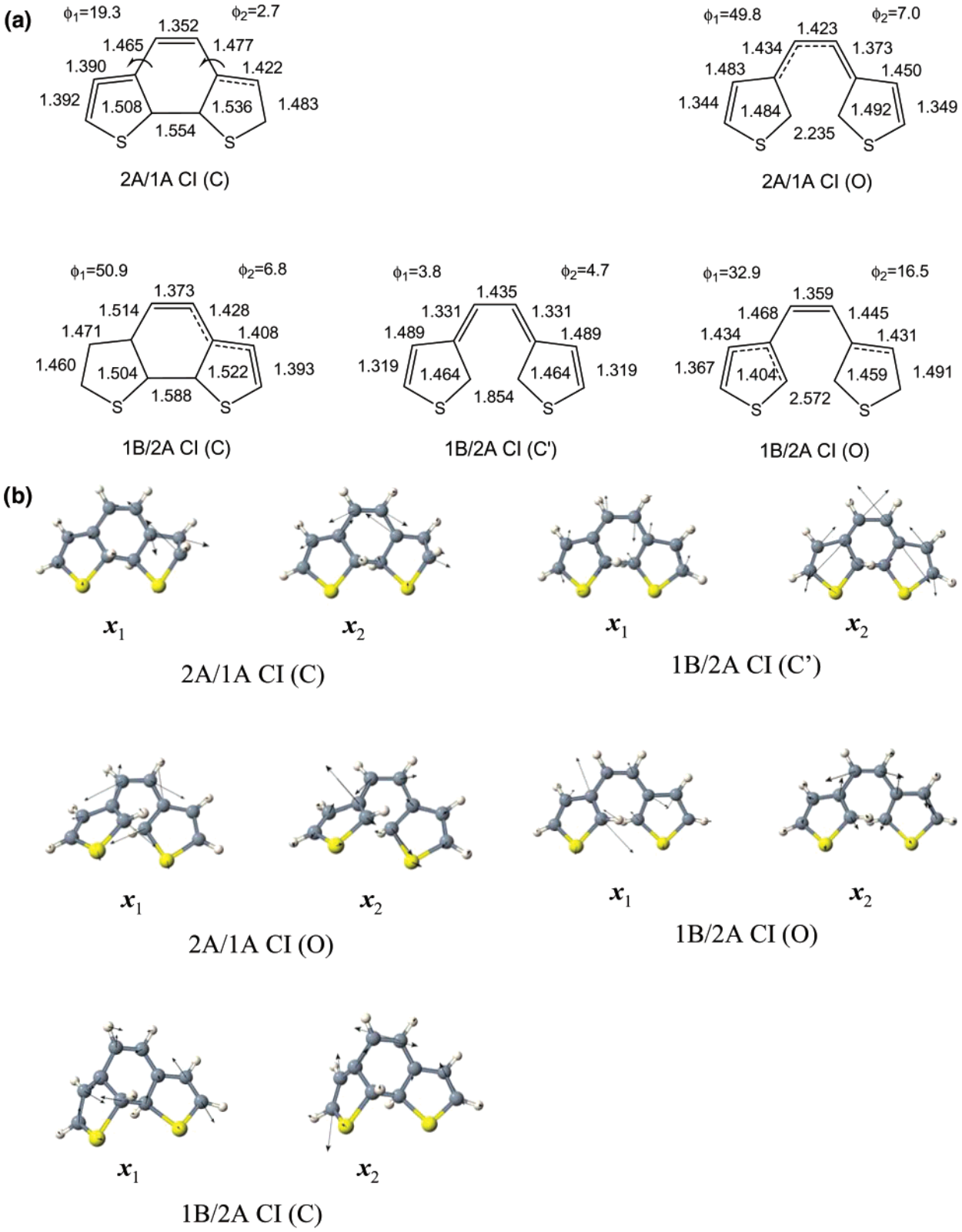

Figure 4. (a) Calculated structures of conical intersections (CIs) for the cycloreversion reaction. The symbol *i*/*j* represents the CI point between the states *i* and *j* in the C_2 symmetry notation, and the letters in parentheses, C and O, represent the closed- and open-ring structures, respectively. The distances between the two carbon atoms are in Å. ϕ_1 and ϕ_2 are the torsion angles about the cyclohexane ring in deg. Here, ϕ_1 and ϕ_2 are different from each other, and the CI structures are distorted from the C_2 symmetry. (b) Two branching vectors: the gradient difference vector $\boldsymbol{x}_1$ and the derivative coupling vector $\boldsymbol{x}_2$ at each conical intersection (CI) point.

(O) point is characterized as a peaked type (along the $\boldsymbol{x}_1$′ direction) in Figure 5b and yielded two products; for example, the MEP to the $1A_C$ was obtained from the CI point itself, while that to the $1A_O$ was calculated from the structure 0.017 Å apart

Table 1. The Relative Energies of the Stationary Points (The Energies Are Relative to the Value of $1A_C$ in kcal/mol)

		method			
		CASSCF	CASSCF	CASSCF	MS-CASPT2[e]
	distance	(10,10)	(10,10)	(14,14)	(10,10)
state	R(C–C)	6-31G	6-31G*	6-31G	6-31G
structure	[Å]	[kcal/mol]	[kcal/mol]	[kcal/mol]	[kcal/mol]
$1A_C$	1.537	0.0[a]	0.0[b]	0.0[c]	0.0[d]
1A TS	2.125	51.6	51.2	49.8	45.4
$1A_O$	3.402	1.2	−2.3	0.6	6.2
2A FC (C)	1.537	110.4	111.4	111.4	97.9
$2A_C$	1.555	81.2	81.0	78.1	71.0
2A TS	1.909	95.4	92.7	91.8	66.3
$2A_O$	2.277	89.4	86.9	87.6	68.6
2A FC (O)	3.402	148.2	144.4	148.5	136.8
1B FC(C)	1.537	135.0	135.2	139.0	76.8
$1B_C$	1.561	111.0	111.1	135.3	68.9
$1B_{C'}$	1.797	122.4	115.7	117.0	59.9
1B TS	2.599	130.5	123.1	126.9	91.2
$1B_O$	4.102	113.1	111.8	118.8	100.4
1B FC(O)	3.402	164.9	146.2	153.2	108.7

[a] CASSCF(10,10)/6-31G energy is relative to −1178.22197 au ($1A_C$). [b] CASSCF(10,10)/6-31G* energy is relative to −1178.42459 au ($1A_C$). [c] CASSCF(14,14)/6-31G energy is relative to −1178.26508 au ($1A_C$). [d] MS-CASPT2(10,10)/6-31G energy is relative to −1179.11188 au ($1A_C$). [e] 1A and 2A states were calculated by the state-specific CASPT2 method, while the 1B state was calculated by the multistate (MS) CASPT2 method with the state-averaged (SA) CASSCF wave functions.

Table 2. The Relative Energies of the Conical Intersections (The Energies Are Relative to the Value of $1A_C$ in kcal/mol; The Values in Parentheses Are the Energy Differences between the Upper and Lower States)

		method		
		SA-CASSCF	SA-CASSCF	MS-CASPT2
	distance	(10,10)	(10,10)	(10,10)
state	R(C–C)	6-31G	6-31G*	6-31G
structure	[Å]	[kcal/mol]	[kcal/mol]	[kcal/mol]
2A/1A CI(C)	1.554	112.5[a]	111.7[b]	92.8[c]
		(0.0)	(2.6)	(2.8)
2A/1A CI(O)	2.235	114.6	114.5	91.1
		(0.0)	(3.7)	(8.9)
1B/2A CI(C)	1.558	125.9	127.4	103.8
		(0.2)	(3.1)	(9.7)
1B/2A CI(C′)	1.854	141.7	137.0	89.2
		(0.1)	(4.6)	(30.0)
1B/2A CI(O)	2.572	128.8	129.4	115.9
		(0.1)	(0.8)	(3.9)

[a] SA-CASSCF(10,10)/6-31G energy is relative to −1178.22197 au ($1A_C$). [b] SA-CASSCF(10,10)/6-31G* energy is relative to −1178.42459 au ($1A_C$). [c] MS-CASPT2(10,10)/6-31G energy is relative to −1179.11188 au ($1A_C$).

Table 3. Conical Parameters of the Conical Intersections Obtained by SA-CASSCF(10,10) Calculations

conical parameter[a]	2A/1A CI(C)	2A/1A CI(O)	1B/2A CI(C)	1B/2A CI(C′)	1B/2A CI(O)
s_x	0.07	0.04	0.05	0.00	−0.10
s_y	−0.14	−0.11	0.07	−0.33	−0.07
g	0.08	0.16	0.01	0.04	0.10
h	0.12	0.11	0.09	0.10	0.07
s^x ($=s_x/g$)	0.83	0.28	8.33	0.04	−0.96
s^y ($=s_y/h$)	−1.15	−1.08	0.79	−3.34	−1.05
d_{gh}	0.11	0.14	0.06	0.08	0.08
Δ_{gh}	−0.35	0.39	−0.99	−0.65	0.41

[a] The definition of the parameters was taken from ref 28a,b.

from the CI point along $\boldsymbol{x}_1$ on the branching plane (Figure 6). As a consequence, this 2A/1A CI (O) point will be a critical point for the cycloreversion reaction. In the next section, we will discuss the reaction mechanism with these CIs taken into consideration.

3.3. Mechanism of the Cycloreversion Reaction. We have reported in the previous paper[21] that the energy difference between the closed- ($2A_C$) and open-ring ($2A_O$) isomers on the 2A state is correlated with the experimental QY of the cycloreversion reaction, where the experimental QY varies as a function of substituents on the same skeleton shown in Scheme 1. It was obtained without the knowledge of CIs. Here, aiming at an understanding of the reaction mechanism through the obtained CIs, we present a further study using the CASSCF PESs. In the next section, we will consider the description based on the CASPT2 energies, especially on the relative energy between the 1B and 2A states.

The outline of the cycloreversion reaction mechanism is shown in Scheme 3. After the excitation to the allowed 1B FC (C) state, the cycloreversion reaction can be achieved through the IC to the doubly excited 2A state, which is linked, in character, to the $1A_O$ ground state. Therefore, the IC onto the 2A surface is a prerequisite. This will occur first with the relaxation from 1B FC(C) to $1B_C$, possibly with the partial vibrational relaxation. The MEP from 1B FC (C) in Figure 2a and b and the geometrical structure relationship in Figure 3 suggest that the 1B state relaxes from the $1A_C$ structure smoothly, keeping the initial R(C−C) bond distance[26] but changing the dihedral angle ϕ halfway to $1B_C$. Continuing the change on one side of the dihedral angle ϕ_1 further with some excess energy, the state will reach the 1B/2A CI (C) point, where the efficient IC to $2A_C$ becomes possible as explained before. Therefore, based on the CASSCF PESs, the first IC from the 1B to 2A state would occur by the induced large amplitude torsional vibration of one thienyl group. The alternative IC path via the 1B/2A CI (O) point would be less plausible because of the large variation in R(C−C) (see Figures 1 and 3).

Although several processes can take place starting from 1B/2A CI(C), all of the MEPs examined from many points on the branching plane led solely to 2Ac as shown in Figure 6. As far as we examined, no MEP to $2A_O$ was obtained;[31] the direct pathway to $2A_O$ may be impossible, which will be discussed later. The energy difference between $2A_C$ and 2A/1A CI(C) is fairly large (31.3 kcal/mol); however, a large excess energy in the torsional motion in ϕ_1 and a geometrical relationship shown in Figure 3 imply that an efficient relaxation from $2A_C$ to $1A_C$ will take place via 2A/1A CI(C).

All of the MEPs from the 2A/1A CI(C) led to $1A_C$ only, as shown in Figure 6. Another possible process starting from $2A_C$ is to pass through 2A TS and populate $2A_O$ by following the intramolecular vibration energy redistribution (IVR) especially from the vibrational motion in the ϕ_1 direction to that in the R(C−C) direction and also the thermal activation by the collisions with solvent molecules. After arriving in the $2A_O$ region, with probable IVR again, the 2A/1A CI (O) state is expected to be reached during the torsional vibration.

For the last step, as the MEPs starting from several points in the branching plane of the 2A/1A CI (O), two types of paths were obtained, arriving at 1Ac and 1Ao, as shown in Figure 6. Thus, after having arrived in the open-ring side on the 2A state

(31) Values of the R(C−C), ϕ_1, and ϕ_2 in these CI structures shown in Figures 3 and 4 suggest that the path from 1B/2A CI (C) to 2A/1A CI (C) consists of the change in the torsion angles (ϕ_1 and ϕ_2). That from 1B/2A CI (C) to 2A/1A CI (O), if it occurs, consists of the R(C−C) changes.

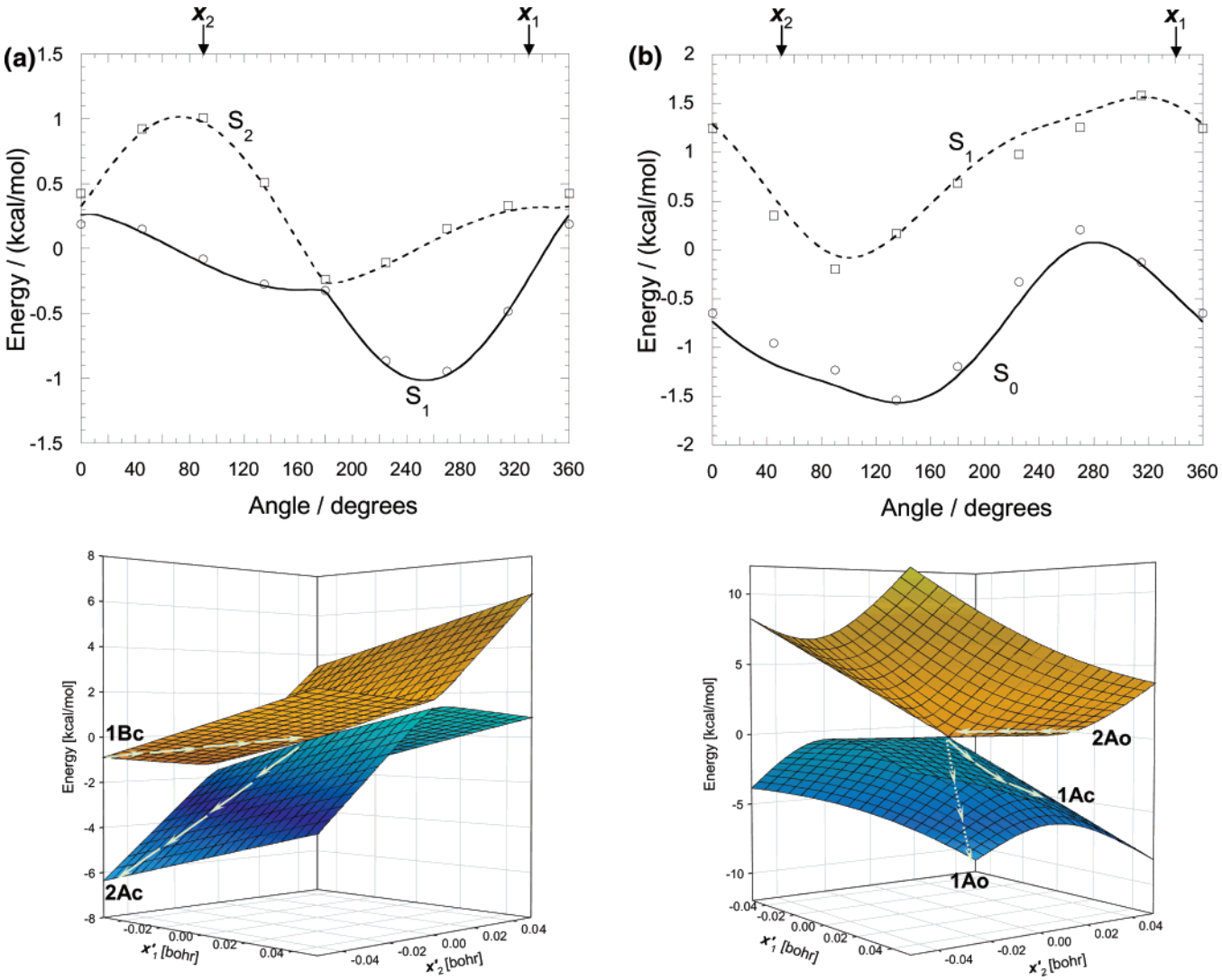

Figure 5. (a) Upper part: Potential energy change along a circle centered at 1B/2A CI(C) with a radius of 0.01 bohr obtained from the actual pointwise CASSCF calculations (S_2, □; S_1, ○) and perturbation theory estimate with conical parameters (S_2, dashed line; S_1, solid line). The $x_{1'}$ direction has been set as 0°. The original x_1 and x_2 directions have been shown by arrows. Lower part: Three-dimensional view of the $S_2(1B)/S_1(2A)$ potential energy surfaces obtained from the perturbation theory, with a representative reaction path. (b) Upper part: Potential energy change along a circle centered at 2A/1A CI(O) with a radius of 0.01 bohr obtained from the actual pointwise CASSCF calculations (S_1, □; S_0, ○) and perturbation theory estimate with conical parameters (S_1, dashed line; S_0, solid line). The $x_{1'}$ direction has been set as 0°. The original x_1 and x_2 directions have been shown by arrows. Lower part: Three-dimensional view of the $S_1(2A)/S_0(1A)$ potential energy surfaces obtained from the perturbation theory, with a representative reaction path.

with excess energy, some of the pathways via the 2A/1A CI (O) can reach the cycloreversion product of 1Ao. Even though the energy difference between $2A_O$ and 2A/1A CI (O) is about the same order as the closed-ring analogue (Tables 1 and 2), QY for the cycloreversion reaction is generally smaller than the direct relaxation to $1A_C$ in the closed-ring side, because the latter does not require the IVR.

As shown in Figure 6, neither from the 1B/2A CI (C) nor from 1B/2A CI (C′), no MEP led to the $2A_O$, to say nothing of the 2A/1A CI (O). This may be because the PES along an MEP should always be downhill and such an MEP does not necessarily represent the actual trajectory. Therefore, the possibility of the direct pathway from the 1B/2A CI (C) to the 2A/1A CI (O) must be examined with a different methodology. Here, as the second best investigation, we have calculated the linear synchronous transit (LST) path,[32] changing all of the geometrical parameters linearly from 1B/2A CI (C) to 2A/1A CI (O), and we show the result in Figure 7. Although the S_1 (2A) energy profile is rather smooth with some barrier (∼20 kcal/mol) and further examination will be needed, we assume that the direct pathway has a negligibly small possibility.

Consequently, the suggested mechanism for the cycloreversion reaction indicates that the IVR and thermal activation processes on the 2A PES in the closed-ring region are crucial. Within this time scale, the cycloreversion reaction then occurs via the 2A/1A CI (O) point. Following the above discussion, the probability of reaching the 2A/1A (C) point will be larger than that of reaching the 2A/1A (O) point. It is also important to note that the 2A/1A CI(O) branching point is located in the open-ring side, outside of 2A TS. These features are consistent with experimental facts that the reported QYs of cycloreversion reactions are rather small relative to those of reverse cyclization reactions (approaching ∼1.0)[3]. Furthermore, the QYs of the cycloreversion reactions increase as the temperature increases.[3,33]

(32) Halgren, T. A.; Lipscomb, W. N. *Chem. Phys. Lett.* **1977**, *49*, 225.

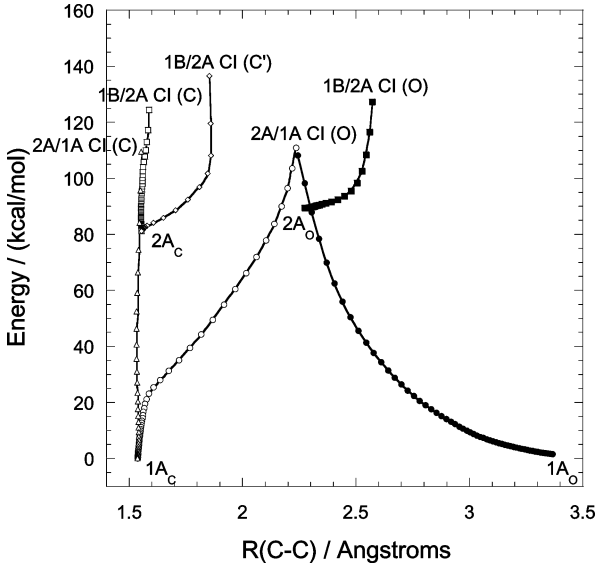

Figure 6. The minimum energy paths (MEPs) from the conical intersection (CI) points. (□): The path from 1B/2A CI (C) to $2A_C$. (◇): The path from 1B/2A CI (C′) to $2A_C$. (■): The path from 1B/2A CI (O) to $2A_O$. (△): The path from 2A/1A CI (C) to $1A_C$. (○): The path from 2A/1A CI (O) to $1A_C$. (●): The path from 2A/1A CI (O) to $1A_O$.

Scheme 3

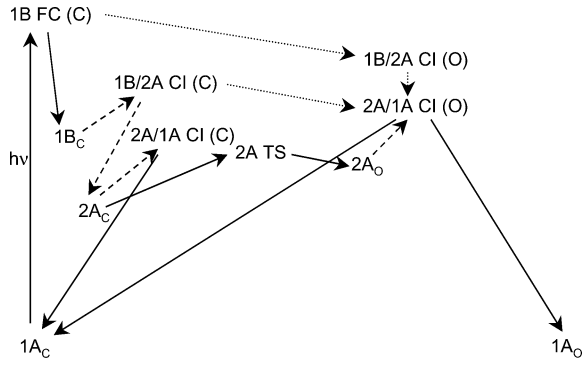

We believe that the correlation of the experimental QYs with the calculated energy difference of $2A_C$ and $2A_O$ is thus explained.[21,34]

3.4. Quality of the Description. To examine the accuracy of the current method, additional calculations were carried out. The results of the single-point calculations using CASSCF (14,14)/6-31G including additional σ orbitals in the active space, CASPT2 (10,10)/6-31G, and CASSCF (10,10)/6-31G* all at the CASSCF (10,10) optimized geometries are shown in Tables 1 and 2. As seen here, the covalent 1A and 2A states are generally well described at the CASSCF(10,10) level, and their PES features including the structures of the 2A/1A CI (C) and 2A/1A CI(O) summarized in Figure 3 will not change significantly at the CASPT2 level. Therefore, most of the main features discussed so far are confirmed, except for the energy of the ionic 1B state, by the CASPT2 level calculations.[35]

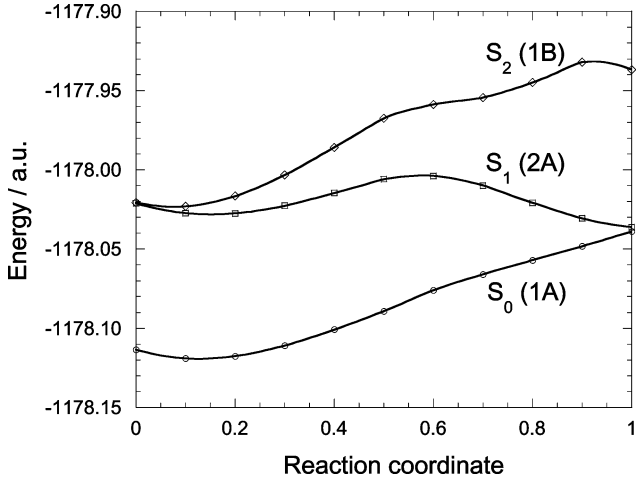

Figure 7. The linear synchronous transit (LST) path[32] from the 1B/2A CI (C) to the 2A/1A CI (O) point. The reaction coordinates of 0 and 1 correspond to 1B/2A CI (C) and 2A/1A CI (O), respectively.

There are some differences: (1) the CASSCF energy of 1B FC(C) is higher than that of 2A FC(C), while the CASPT2 energy of 1B FC(C) is lower, (2) CASSCF gives the $1B_C$ minimum (Figure 1), while no 1B minimum appears in this region at the nonoptimized CASPT2 level,[36] and (3) the 2A TS and 1B TS disappeared at the same CASPT2 level.

Preliminary CASPT2 study suggests that a 1B/2A CI of C_2 symmetry (a real crossing) should exist between the FC and intermediate regions; therefore, rapid decay from the 1B FC(C) to 2A state is possible via the 1B/2A CI. This rapid decay from the 1B (bright) to 2A (dark) state could be the reason why little fluorescence has been observed in practice.[37] Although the location and characterization of this 1B/2A CI at the CASPT2 level will be an important future subject, there is a high possibility that the relaxation starts via this 1B/2A CI. Because the geometrical (Figure 3) and energetic (Tables 1 and 2) relationships among the several key states on the 1A and 2A PESs, for example, $1A_C$, 2A/1A CI (C), and 2A/1A CI (O), will not change significantly at the CASPT2 level, the cycloreversion reaction mechanism considered previously based on the 2A CASSCF PES is expected to apply equally. Even though $2A_O$ is populated via the 1B/2A CI, the rate to reach 2A/1A CI (O) would be considerably slow, because of the slow IVR process on going from the closed- to open-ring structure on the 2A PES.

In Table 1, the nonoptimized CASPT2 energies on the CASSCF geometries suggest that the TS on the 2A PES disappeared. However, this does not change or even favor the picture of the IVR-induced cycloreversion mechanism via 2A/1A CI (O).[38] It is noted that large and about the same energy

(33) (a) Irie, M.; Lifka, T.; Kobatake, S.; Kano, N. *J. Am. Chem. Soc*. **2000**, *122*, 4871. (b) Nakamura, S.; Kanda, K.; Guillaumont, D.; Uchida, K.; Irie, M. *Nonlinear Opt.* **2000**, *26*, 201.

(34) According to the correlation diagram obtained previously (ref 21), the QY of the current compound is expected to be relatively small (~0.01) because the energy difference is 8.3 kcal/mol (1 kcal/mol = 0.043364 eV).

(35) For the correct evaluation of the 1B relative to 2A state, the CASSCF level is believed not to be sufficient, as reported in many studies of polyenes. For example: Nakayama, H.; Hirao, K. *Int. J. Quantum Chem*. **1998**, *66*, 157 and references therein.

(36) At the CASSCF level, the electronic characters of the 1B and 2B states are interchanged along R(C−C) near 1.8 Å which causes the $1B_C$ minimum, while at the CASPT2 level there is no such interchange and the character of 1B is kept as HOMO → LUMO excitation along R(C−C).

(37) (a) Kim, M. S.; Kawai, T.; Irie, M. *Chem. Lett*. **2001**, *30*, 702. (b) Kim, M. S.; Kawai, T.; Irie, M. *Opt. Mater*. **2002**, *21*, 271. (c) Yagi, K.; Irie, M. *Chem. Lett*. **2003**, *32*, 848.

(38) If the feature of the PES, no TS on the 2A surface, at the preliminary nonoptimized CASPT2 level is correct, the reason for the small QYs of the cycloreversion relative to the cyclization reaction, and the temperature dependency of the former reaction, might be attributed to other unknown mechanisms such as the difference of microscopic density of state between the 2A/1A CI (C) and 2A/1A CI (O), or the existence of some vibrational promoting modes on the 2A surface. Such detailed studies are important future subjects for experiments and theory.

differences exist between $2A_C$ ($2A_O$) and 2A/1A CI(C) (2A/1A CI(O)) (see Tables 1 and 2) both at the CASSCF and at the CASPT2 levels. If the IVR process is very efficient, and 2A TS does not exists, we naturally expect the same order of the rates to reach 2A/1A CI (C) and 2A/1A CI (O), about the same order of QYs for the closed- and open-ring products, which contradicts the experimental observation.

Taking the dynamical electron correlation into account at the CASPT2 level, the initial decay process from 1B to 2A and consequently the probability of reaching $2A_O$ will probably be corrected, and also the PES features for the 2A state as well as the 1B state may be modified; nevertheless, the quasi-equilibration or IVR-induced cycloreversion mechanism via 2A/1A CI (O) is expected to be a common picture to the CASSCF and CASPT2 levels. Detailed features such as the optimization of CIs and the transition states at the CASPT2 level are future subjects.

4. Conclusion

Photochromic dithienylethene molecules have a wealth of potential for future molecular devices. As an extension of the previous study, in which the correlation of QYs with the energy difference of the $2A_C$ and $2A_O$ states in the cycloreversion reaction was reported,[21] a theoretical study on the model system of dithienylethenes has been presented to explore further the detailed mechanisms of the photochromic cycloreversion reactions. The structures of CIs were obtained, and their role was discussed using the CASSCF method. The mechanism with IVR-induced (from the $\pi \rightarrow \pi^*$ excitation-generated torsion modes to the ring-opening C−C stretching modes) cycloreversion toward the quasi-equilibrium on the 2A surface was proposed, consistent with experimental facts of small QYs and their temperature dependency.

Acknowledgment. We thank Profs. K. Uchida, H. Miyasaka, H. Sekiya, Drs. S. Kobatake, K. Kanda, and G. Treboux for discussions. This work was supported by ACT-JST. S.Y. was supported by a Grant-in-Aid for the 21st Century COE program "KEIO LCC" from the Ministry of Education, Culture, Sports, Science, and Technology, Japan.

JA035035O